Scanning Microscopy

9-3-1996

Monte Carlo Simulation of Electron Backscattering in Solids Using a General-Purpose Computer Code

E. Acosta
Universidad Nacional de Córdoba, eduardo@quechua.fis.uncor.edu

E. Coleoni
Universidad Nacional de Córdoba

G. Castellano
Universidad Nacional de Córdoba

J. A. Riveros
Universidad Nacional de Córdoba

J. M. Fernández-Varea
Universitat de Barcelona

See next page for additional authors

Follow this and additional works at: https://digitalcommons.usu.edu/microscopy

Part of the Biology Commons

Recommended Citation

Utah State University
MERRILL-CAZIER LIBRARY

Monte Carlo Simulation of Electron Backscattering in Solids Using a General-Purpose Computer Code

Authors

E. Acosta, E. Coleoni, G. Castellano, J. A. Riveros, J. M. Fernández-Varea, and F. Salvat

MONTE CARLO SIMULATION OF ELECTRON BACKSCATTERING IN SOLIDS USING A GENERAL-PURPOSE COMPUTER CODE

E. Acosta[1,*], E. Coleoni[1], G. Castellano[1], J.A. Riveros[1], J.M. Fernández-Varea[2] and F. Salvat[1,2]

[1]Facultad de Matemática, Astronomía y Física, Universidad Nacional de Córdoba,
Medina Allende y Haya de la Torre, 5000 Córdoba, Argentina
[2]Facultat de Física (ECM), Universitat de Barcelona, Barcelona, Spain

Abstract

A Monte Carlo study of backscattering of kilovolt electrons in solids, a process of primary importance in electron microscopy and surface analytical techniques, is carried out. Simulations have been performed using the general-purpose simulation code PENELOPE (an acronym for "Penetration and ENErgy LOss of Positrons and Electrons"), which generates electron-photon showers in arbitrary materials. A systematic comparison of results from PENELOPE with available experimental data, and with results from simulations with a much more sophisticated code, is given for electron beams with energies between 2.5 and 60 keV and elemental solids with atomic numbers $Z = 4$ to 92. It is concluded that PENELOPE gives a reliable description of the backscattering process, even for relatively low electron energies and thin targets.

*Contact for correspondence:
Eduardo R. Acosta, address as above.
   Telephone number: 54-51-334051/52/55
     FAX number: 54-51-334054
   E.mail: eduardo@quechua.fis.uncor.edu

Introduction

Electrons impinging on the surface of a solid target undergo a succession of scattering processes within the solid and as a result, a fraction of them return to the surface and escape from the target. A reliable description of the number and the angle-energy distribution of these backscattered electrons is required for quantization in scanning electron microscopy (SEM), electron probe microanalysis (EPMA), Auger electron spectroscopy (AES), etc. Simple theories have been formulated to describe electron backscattering on the basis of either a single-scattering model (Everhart, 1960), approximate diffusion models (Archard, 1961; Thümmel, 1974) or combinations of both (Niedrig, 1981). These simple theories can only reproduce the gross features of backscattering. A more realistic description can be obtained by numerically solving the Boltzmann transport equation (Fathers and Rez, 1979). However, the solution of this integro-differential equation poses considerable difficulties and is feasible only for relatively simple interaction models. Monte Carlo simulation methods (Kalos and Whitlock, 1986) are well suited for studying radiation transport processes, and have been widely used in the past to study electron backscattering in solids (Shimizu and Murata, 1971; Reimer and Krefting, 1976; Liljequist, 1983a; Martínez et al., 1990). The practical advantage of Monte Carlo methods is that they can implement realistic interaction models and can be applied to arbitrary geometries (e.g., multilayer samples, tilted specimens, converging beams, etc.).

A Monte Carlo method is defined by the adopted scattering model (i.e., the set of cross sections for the different interaction mechanisms) and simulation algorithm (the set of rules used to generate random electron tracks from a given scattering model). For kV electrons, "detailed" algorithms, which simulate all interactions along a track in chronological succession, are applicable. Detailed simulation is nominally exact, i.e., it yields results that, apart from the inherent statistical uncertainties, agree with those that would be obtained from the solution of the Boltzmann transport equation with the

same scattering model. Since the number of collisions experienced by an electron until it comes to rest increases with its initial energy, detailed algorithms are very inefficient for electrons with high initial energies. The majority of high-energy simulation codes (Jenkins *et al.*, 1988) implement "condensed" algorithms (Berger, 1963), which generate the global effect of the interactions along a track segment of a given length in a single computational step with the aid of multiple scattering theories. These theories introduce approximations that may affect the simulation results (Bielajew and Rogers, 1987). A more satisfactory approach is provided by the so-called "mixed" simulation algorithms (Fernández-Varea *et al.*, 1993) that combine (exact) detailed simulation of hard interactions (i.e., interactions with scattering angle or energy loss greater than given cutoff values) with condensed simulation of soft interactions. If the angle and energy cutoffs are properly selected, mixed simulation is as accurate as detailed simulation and may represent a considerable economy in computer time, even for relatively low energies. Nevertheless, mixed simulation of both elastic and inelastic scattering has only been occasionally used for kV electrons (e.g., by Reimer and Krefting, 1976).

The first simulations of kilovolt electron transport were based on very simple scattering models. Thus, in the early eighties, it was a common practice to use the screened Rutherford cross section to describe elastic collisions and to rely on the continuous slowing down approximation to simulate energy losses. Since then, most of the simulation work in the kV energy range has been concentrated in demonstrating the reliability of scattering models of increasing complexity using detailed simulation algorithms. In spite of the success of these Monte Carlo methods, systematic studies of electron backscattering covering a wide spectrum of materials, energies and directions of incidence are scarce. The main reason for the lack of systematic simulation studies is that to obtain accurate cross sections one must perform quite elaborate calculations, specific of each material. Moreover, these cross sections are usually obtained in numerical form and this considerably complicates the simulation code, which must work on the basis of interpolation in extensive data tables.

In this paper, the general-purpose simulation package PENELOPE (an acronym for "Penetration and ENErgy LOss of Positrons and Electrons", Baró *et al.*, 1995) is applied to the study of electron backscattering in solids. PENELOPE implements a mixed simulation algorithm that was initially developed to generate electron-photon showers in arbitrary material systems for a wide energy range, from ~1 GeV down to ~100 eV. Condensed Monte Carlo codes, e.g., EGS4 (Nelson *et al.*, 1985), ETRAN (Berger and Seltzer, 1988), which

are of common use in dosimetry and medical physics, are not applicable to kilovolt electrons because of the approximations introduced by the multiple scattering theories implemented in those codes. Our objective here is to evidence that PENELOPE gives a reliable description of kilovolt electron backscattering and, therefore, can be adopted as a routine tool, e.g., to compute backscattering factors for quantitative analysis with EPMA and AES. Benchmark comparisons of simulation results with a variety of experimental data from the literature are presented. This kind of systematic analysis represents a necessary step prior to the use of any simulation code for practical quantitation purposes. The source files and interaction database of PENELOPE are available from the authors upon request.

The Simulation Algorithm

PENELOPE is a self-contained simulation code (Baró *et al.*, 1995; Sempau *et al.*, submitted) developed to generate electron-photon showers in material systems consisting of a number of homogeneous bodies limited by well-defined surfaces. PENELOPE is applicable to electrons and positrons with energies higher than a few hundred eV and to photons with energies above 1 keV. In what follows, we will concentrate on the transport of kilovolt electrons; the parts of the computer code that simulate positrons and photons have no effect for the kind of problems considered here.

Scattering model

The considered interactions are elastic scattering and inelastic collisions; bremsstrahlung emission is also accounted for by PENELOPE, but has a negligible stopping effect for electrons with energy E less than ~100 keV. Electron tracks are generated by means of a mixed algorithm with automatically selected cutoffs. For the sake of completeness, the adopted atomic differential cross sections (DCSs) are outlined below. In the case of compound materials, molecular DCSs are obtained using the additivity approximation, i.e., as the sum of the atomic DCSs of the elements present. Details on the theory underlying the Monte Carlo algorithm and a global analysis of the reliability of simulation results have been published elsewhere (Baró *et al.*, 1995).

Inelastic collisions: The effect of individual inelastic collisions on the projectile is described by the energy loss W and the recoil energy Q, defined by

$$Q = \frac{(p - p')^2}{2m} \qquad (1)$$

where **p** and **p'** are the linear momenta of the swift electron before and after the collision and m is the electron

mass. The DCS for inelastic collisions σ_{col} derived from the non-relativistic first Born approximation can be written in the form

$$\frac{d^2\sigma_{col}}{dWdQ} = \frac{2\pi e^4}{mv^2}\frac{1}{WQ}\frac{df(Q,W)}{dW} \qquad (2)$$

where v is the velocity of the projectile and e is the electron charge. The function $df(Q,W)/dW$ is the generalized oscillator strength (GOS), which is studied in detail by Inokuti (1971).

To obtain the collision DCS in analytical form, the simple GOS model proposed by Liljequist (1983b) is adopted. In this model, the response of the target to inelastic collisions is represented by a limited number M of excitations (or undamped classical oscillators) characterized by resonance energies W_i and oscillator strengths f_i. The Liljequist GOS can be written as

$$\frac{df(Q,W)}{dW} = \sum_{i=1}^{M} f_i F(W_i;Q,W) \qquad (3)$$

The excitation spectrum $F(W_i;Q,W)$ of the i-th oscillator is assumed to be

$$F(W_i;Q,W) = \delta(W - W_i)\theta(W_i - Q) \\ + \delta(W - Q)\theta(Q - W_i) \qquad (4)$$

where $\delta(x)$ is the Dirac delta function and $\Theta(x)$ is the step function. In the limit of small momentum transfers, the GOS reduces to the optical oscillator strength (OOS),

$$\frac{df(Q=0,W)}{dW} = \sum_{i=1}^{M} f_i\delta(W-W_i) \qquad (5)$$

which has the same analytical form as the OOS underlying Sternheimer's calculations of the density effect correction (Sternheimer, 1952). In order to reproduce the high-energy stopping power given by the Bethe formula (Berger and Seltzer, 1982), the excitation energies and oscillator strengths must satisfy the following "sum rules"

$$\sum f_i = Z; \\ \sum f_i \ln W_i = Z\ln I \qquad (6)$$

where I denotes the mean excitation energy, the central parameter in the Bethe stopping power formula.

Following Sternheimer (1952), excitations of each atomic electron shell are described by means of a single oscillator. We set

$$f_i = Z; \\ W_i = \sqrt{(aU_i)^2 + \frac{2}{3}\frac{f_i}{Z}\Omega_p^2} \qquad (7)$$

where Z_i is the number of electrons in the i-th shell, U_i is their ionization energy and Ω_p is the plasma energy corresponding to the total electron density in the material, and a is a semiempirical adjustment factor. The term $2f_i\Omega_p^2/3Z$ under the square root in eq. (7) accounts for the Lorentz-Lorenz correction. Plasmon excitations are described by a single oscillator with binding energy $U_p = 0$, resonance energy W_p and oscillator strength f_p. The parameters W_p and f_p should be identified with the plasmon energy and the effective number of electrons that participate in plasmon excitations (per atom). These quantities can be deduced, e.g., from electron energy-loss spectra or from measured optical data. When this information is not available, we can simply fix the value of f_p and set $W_p = (f_p/Z)^{1/2}\Omega_p$. This prescription was used by Sternheimer et al. (1984) to calculate the density effect correction for single-element metals; f_p was taken to be the lowest chemical valence of the element. In practice, the values of W_p and f_p have little influence on the stopping power for energies E larger than a few keV. For instance, in the case of aluminium, the relative difference between the stopping powers computed with $f_p = 3$ and with $f_p = 0$ is less than 1% for $E = 500$ eV and decreases rapidly with increasing energies.

The semiempirical adjustment factor a in eq. (7) is introduced to obtain agreement with the adopted mean excitation energy I. It is obtained as the positive root of the equation

$$Z\ln I = f_p\ln W_p \\ + \sum f_i\ln\sqrt{(aU_i)^2\frac{2}{3}\frac{f_i}{Z}\Omega_p^2} \qquad (8)$$

PENELOPE uses the ionization energies U_i given by Lederer and Shirley (1978). The default mean excitation energies I of the elements are the ones recommended by Berger and Seltzer (1982). Exchange, relativistic, and density effect corrections are introduced as described by Salvat and Fernández-Varea (1992).

Excitations of a given oscillator correspond to ionizations of the associated atomic electron shell. It is assumed that as the result of an inelastic collision with the i-th oscillator, a secondary electron is emitted with initial energy $W - U_i$ in the direction of the momentum transfer. Secondary electrons with initial energy larger than the absorption energy E_{abs} adopted in the simulation (100 eV in the present calculations) are followed after completing the simulation of the primary electron track.

627

Elastic scattering: Elastic scattering is simulated by means of the W2D model described by Baró *et al.* (1994). This model is based on a simple analytical DCS, $d\sigma_{el}/d\Omega$, depending on three parameters. It takes advantage of the fact that angular and spatial distributions after multiple scattering are completely determined by a few integral properties of the single scattering DCS. Of course, when the number of scattering events is small (plural scattering), the angular and spatial distributions reflect the fine details of the DCS, but these are washed out after a sufficiently large number of collisions. An interesting demonstration of this idea applied to electron backscattering has been given by Liljequist (1983a).

The quantities of primary importance in plural and multiple elastic scattering are the total cross section

$$\sigma_{el} = \int \frac{d\sigma_{el}}{d\Omega} d\Omega \qquad (9)$$

the first transport cross section

$$\sigma_1 = \int (1 - \cos\theta) \frac{d\sigma_{el}}{d\omega} d\omega \qquad (10)$$
$$= \sigma_{el}(1 - <\cos\theta>)$$

and the second transport cross section

$$\sigma_2 = \int \frac{3}{2}(1 - \cos^2\theta) \frac{d\sigma_{el}}{d\Omega} d\Omega \qquad (11)$$
$$= \sigma_{el}\frac{3}{2}(1 - <\cos^2\theta>)$$

where θ is the polar scattering angle and $<\cdot>$ indicates the average value in a single collision. These integrated cross sections have been calculated for the elements $Z = 1$ to 92 using the PWADIR code (Salvat and Mayol, 1993), which performs a partial wave analysis of the Dirac electron wave function for the Dirac-Hartree-Fock-Slater self-consistent atom field (Salvat *et al.*, 1987), corrected for exchange and solid-state effects.

The analytical form of the W2D DCS corresponds to a combination of a simple screened Rutherford process, which is physically plausible, and a fixed-scattering-angle process that normally represents a small correction. Explicitly,

$$\frac{d\sigma_{W2D}}{d\Omega} = \frac{\sigma_{el}}{4\pi}\left[\frac{4A(1+A)(1-B)}{(1-\cos\theta+2A)^2} \right.$$
$$\left. + B\delta(\cos\theta - \cos\theta_0) \right] \qquad (12)$$

The angle θ_0 is a function of the parameters A and B, which in turn are determined by requiring that the ac-

cepted values of σ_1 and σ_2 are exactly reproduced; notice that the integral of eq. (12) gives σ_{el}, as required. The form (12) was selected to meet certain simplicity requirements needed to formulate the mixed simulation algorithm. Indeed, the precise form of the adopted DCS is quite irrelevant and similarly accurate results could be obtained with any DCS that reproduces the accepted values of the integrals of eqs. (9)-(11) (see, e.g., Fernández-Varea *et al.*, 1991).

It has been shown (Baró *et al.*, 1994) that the W2D model leads to essentially the same multiple scattering distributions as the partial wave DCS. The key point is that such a simple model permits a considerable reduction in the required numerical information: instead of the DCS, a function of the energy *and* the scattering angle, we only need the total and transport cross sections, three functions of the energy. These functions give smooth curves when plotted in a log-log representation. They have been tabulated for a logarithmic grid of energies from which accurate values are obtained by log-log cubic spline interpolation. An extra advantage of the W2D model as compared with numerical DCSs is that the sampling of the scattering angle in individual collisions is done in a purely analytical way, which is much faster than numerical sampling methods.

PENELOPE is coded as a FORTRAN 77 subroutine package, which performs the physical part of the simulation. It dictates the path length to the following interaction event, the kind of interaction that takes place, the energy loss and the change in direction of movement of the particle and the production of secondary electrons. A main program, which controls the evolution of the tracks and keeps score of the relevant quantities, must be provided by the user for each specific geometry. In the present simulations, we have used a main program adapted to multilayer geometries and axially symmetric electron beams. This program yields very detailed information of the transport process, including angular and energy distributions of backscattered and transmitted electrons, depth-dose functions, etc.

Backscattering Coefficient

The backscattering coefficient η is defined as the average number of electrons that are ejected from the irradiated surface per incident electron. Evidently, η is a function of the beam energy, the angle of incidence relative to the surface normal and the composition of the sample. The definition of the backscattering coefficient includes the contribution of secondary electrons. In experimental measurements, this contribution is partially suppressed by applying a positive potential to the sample or by means of retarding grids placed between the sample and the detector. Thus, experimental measurements
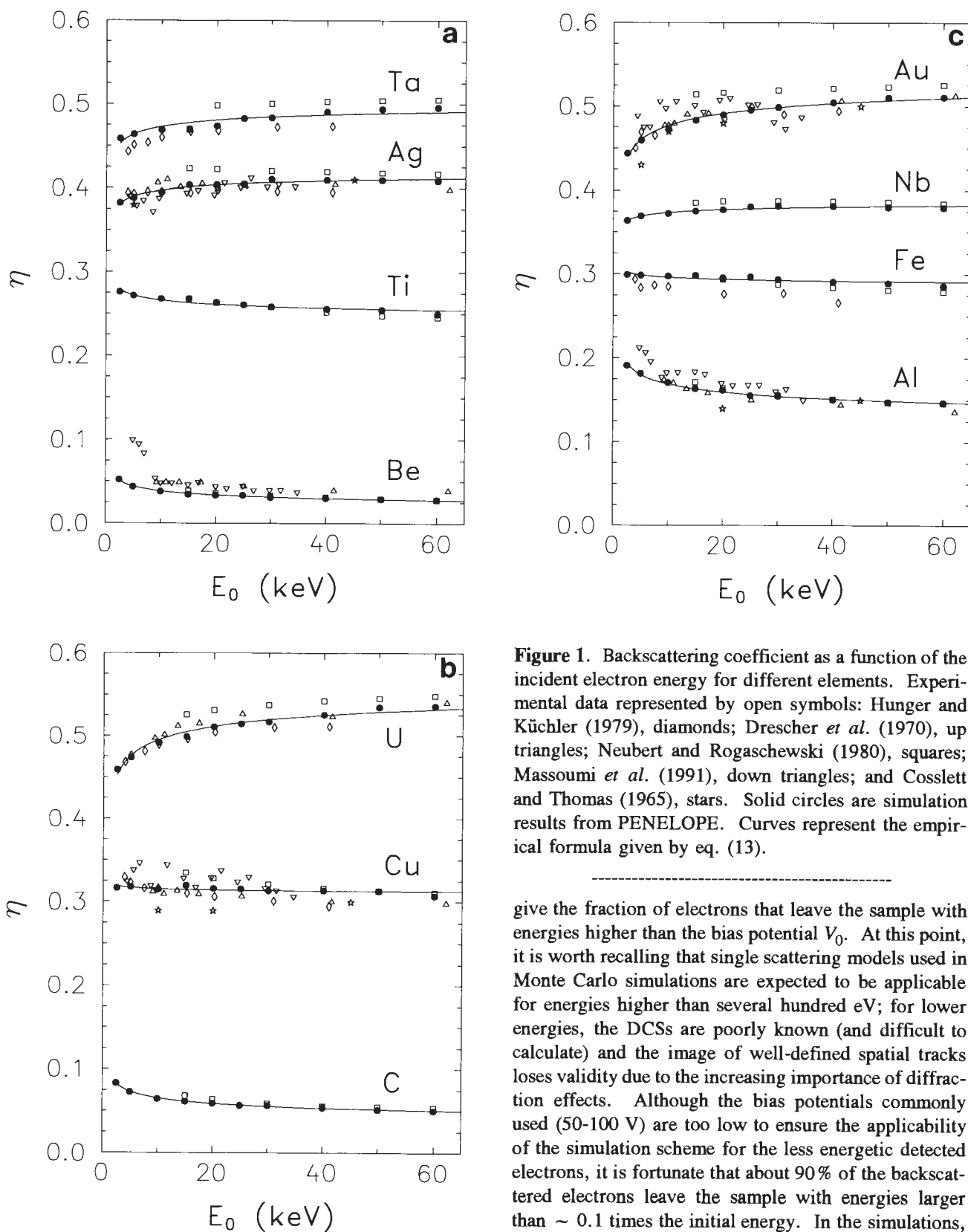
Figure 1. Backscattering coefficient as a function of the incident electron energy for different elements. Experimental data represented by open symbols: Hunger and Küchler (1979), diamonds; Drescher *et al.* (1970), up triangles; Neubert and Rogaschewski (1980), squares; Massoumi *et al.* (1991), down triangles; and Cosslett and Thomas (1965), stars. Solid circles are simulation results from PENELOPE. Curves represent the empirical formula given by eq. (13).

----

give the fraction of electrons that leave the sample with energies higher than the bias potential V_0. At this point, it is worth recalling that single scattering models used in Monte Carlo simulations are expected to be applicable for energies higher than several hundred eV; for lower energies, the DCSs are poorly known (and difficult to calculate) and the image of well-defined spatial tracks loses validity due to the increasing importance of diffraction effects. Although the bias potentials commonly used (50-100 V) are too low to ensure the applicability of the simulation scheme for the less energetic detected electrons, it is fortunate that about 90 % of the backscattered electrons leave the sample with energies larger than ~ 0.1 times the initial energy. In the simulations, we assume that electrons are effectively stopped and absorbed in the medium when their energy falls below 100 eV; differences between this value and the actual bias

Table 1. Parameters of the analytical formula, eq. (13), for the backscattering coefficient, fitted for E_0 ranging from 2.5 to 60 keV.

Z		$a_1(Z)$	$a_2(Z)$
4	Be	8.229E-3	7.563E-2
6	C	2.419E-2	6.868E-2
13	Al	1.092E-1	4.486E-2
22	Ti	2.350E-1	1.415E-2
26	Fe	2.818E-1	5.566E-3
29	Cu	3.071E-1	2.866E-3
41	Nb	3.964E-1	-5.618E-3
47	Ag	4.359E-1	-8.244E-3
73	Ta	5.211E-1	-6.617E-3
79	Au	5.667E-1	-1.137E-2
92	U	5.964E-1	-1.103E-2

potential generally cause very small systematic deviations between the simulated backscattering coefficient and experimental data.

Backscattering coefficients at normal incidence, for a grid of primary electron energies between 2.5 keV and 60 keV, have been computed from simulations for 11 elements covering the periodic table. The simulation code is relatively fast, even when run on personal computers, and could be significantly improved by using variance reduction techniques (see, e.g., Bielajew and Rogers, 1988), which have not been considered in the present analysis. The simulations reported here were performed on 80486 DX2 (66 MHz) IBM-compatible personal computers; typical simulation speeds are of the order of 3-15 tracks per second, including the simulation of secondaries. The number of primary tracks generated in each run was large enough to ensure that the statistical uncertainty of the backscattered fraction (three standard deviations) be less than 1%. To achieve this requirement, a number of the order of 300,000 tracks had to be simulated for low atomic number elements.

In Figure 1, simulated backscattering coefficients are compared with experimental data from different authors. The agreement is seen to be satisfactory, especially for those elements for which data measured by various groups are available. In fact, we have limited the present study to backscattering not only because of the basic importance of this process but also because of the availability of measurements from independent laboratories. The spread of experimental data indicates that these are affected by instrumental uncertainties (sample preparation, beam instabilities, etc.) and, therefore, a comparison with measurements from a single laboratory
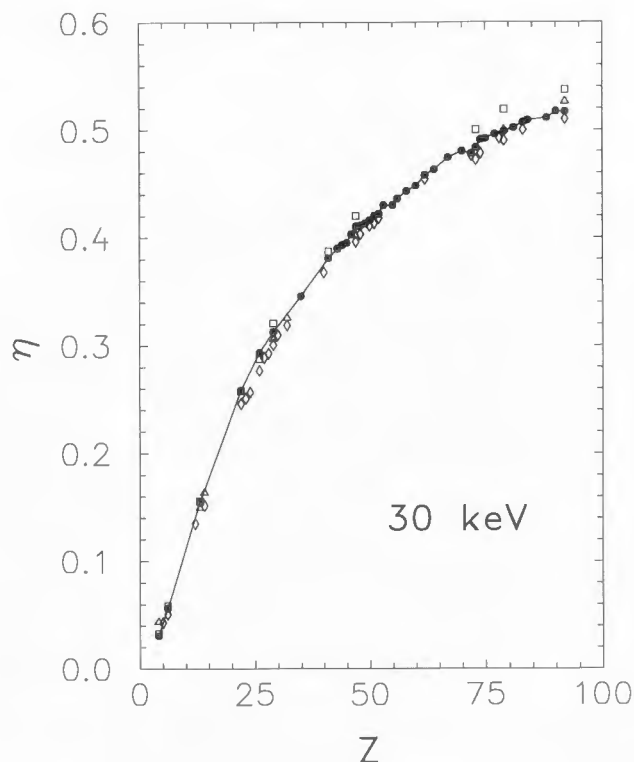

Figure 2. Backscattering coefficient versus atomic number Z for 30 keV electrons at normal incidence. Open symbols are experimental data from different sources: Hunger and Küchler (1979), diamonds; Drescher *et al.* (1970), up triangles; Neubert and Rogaschewski (1980), squares. Solid circles represent results from PENELOPE, joined by straight segments for visual aid, the error bars (three standard deviations) are of the same size as the symbols.

---

may not be conclusive (a fact frequently disregarded in the literature). In some cases, the small systematic differences between simulation and the set of experimental data from a laboratory could be attributed to the aforesaid difference between the experimental bias potential and the Monte Carlo absorption energy. Unfortunately, not all authors quote the adopted bias potential, so that a deeper analysis of this point is not possible.

As Monte Carlo results are only affected by statistical uncertainties, and this can be made as small as needed, simulated data provide a convenient basis for analytical formulae. The continuous curves in Figure 1, represent the function

$$\eta(Z,E_0) = a_1(Z) + a_2(Z)ZE_0^{-1/4} \qquad (13)$$

where E_0 is given in eV. The parameters a_1 and a_2, determined by numerical fitting of the simulated backscattering coefficient of each element are given in Table 1.
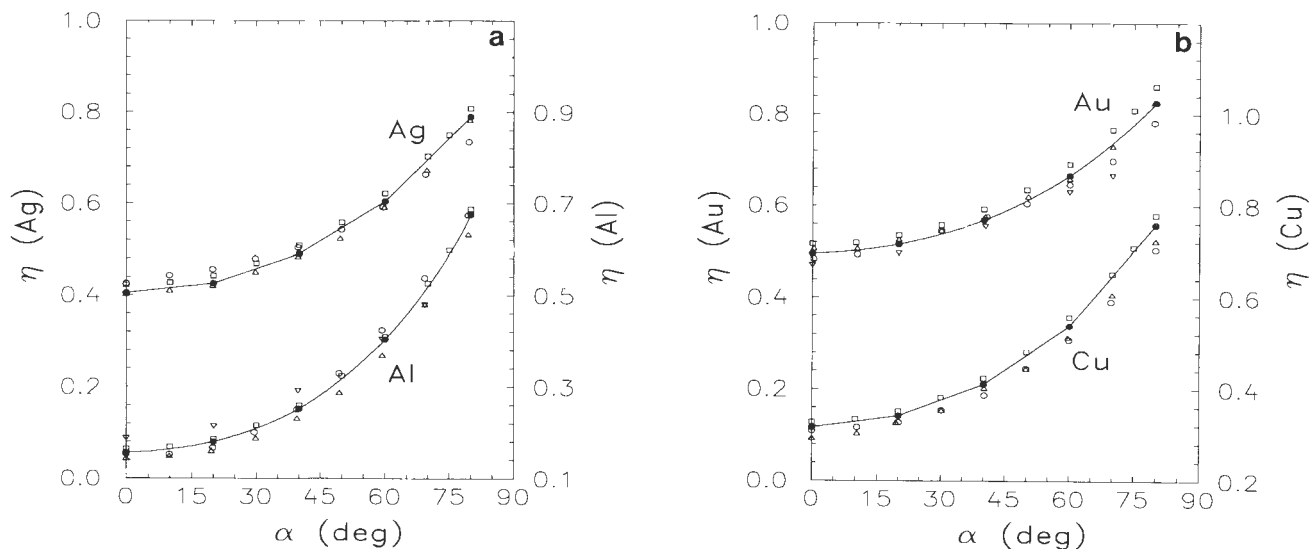
Figure 3. Backscattering coefficient as a function of angle of incidence relative to the surface normal. Open symbols represent experimental data from several authors: Drescher *et al.* (1970), up triangles; Nakhodin *et al.* (1962), down triangles; and Kanter (1957), open circles. Solid circles are results from PENELOPE, joined with straight segments for visual aid. The beam energy used in the simulations and in the aforesaid experiments was $E_0 = 25$ keV. Measurements of Neubert and Rogaschewski (1980), represented with open squares, were performed with $E_0 = 20$ keV.

Figure 2 displays simulated and measured backscattering coefficients for 30 keV electrons at normal incidence as a function of atomic number. This figure is illustrative of the fact that, although the backscattering coefficient for a given material varies monotonously with the energy of the incident beam, the variation with Z (for a given E_0) is not continuous but fluctuates about a smooth curve. These fluctuations, which arise from the non-monotonous behaviour of the elastic and inelastic DCSs as functions of the atomic number, limit the accuracy attainable with empirical analytical formulae for $\eta(Z,E_0)$. Conversely, simple backscattering theories that yield analytical expressions for $\eta(Z,E_0)$, and thus predict a continuous variation of the backscattering coefficient with Z, can be quite accurate for some elements but will necessarily introduce errors of the order of these "natural" fluctuations for other elements (those that depart from the smooth behaviour).

Variation with angle of incidence

Owing to the approximate nature of the elastic DCS, PENELOPE provides a good description of backscattered electrons that have suffered a large number (say > 15) of elastic scattering events. However, a fraction of electrons, those which contribute to the quasielastic peak, are backscattered after a single or very few elastic collisions (single or plural scattering) with small energy losses. As the DCS is strongly peaked at small scattering angles, the number of backscattered electrons that have only undergone plural scattering increases with the

angle of incidence (i.e., when the specimen is tilted relative to the incident beam). Thus, the variation of the backscattering coefficient with the angle of incidence offers a stringent test for the validity of the elastic scattering model.

The backscattering coefficients for 25 keV incident beams and four different materials are displayed in Figure 3, as functions of the angle of incidence α relative to the surface normal ($\alpha = 0$ for normal incidence). It is seen that, on average, simulation results agree well with experimental data taken from different authors, even for relatively large incidence angles. We do not observe any trend of the simulation results to deviate from the experiments at large angles.

Variation with sample thickness

For thin foils, the backscattering coefficient increases monotonously with thickness to reach the saturation value, the bulk backscattering coefficient, for foil thicknesses of the order of half the Bethe range, i.e., the mean path length obtained from the continuous slowing down approximation. This fact can be used to measure the thickness of thin foils (Niedrig, 1982).

It is important to recall that the W2D model is only applicable for multiple scattering, i.e., when the average number of elastic collisions per electron track is of the order of 15 or larger. Therefore, simulation with PENELOPE should be limited to films thick enough to satisfy this requirement. Fortunately, this is not too strong a limitation and the simulation can be applied to
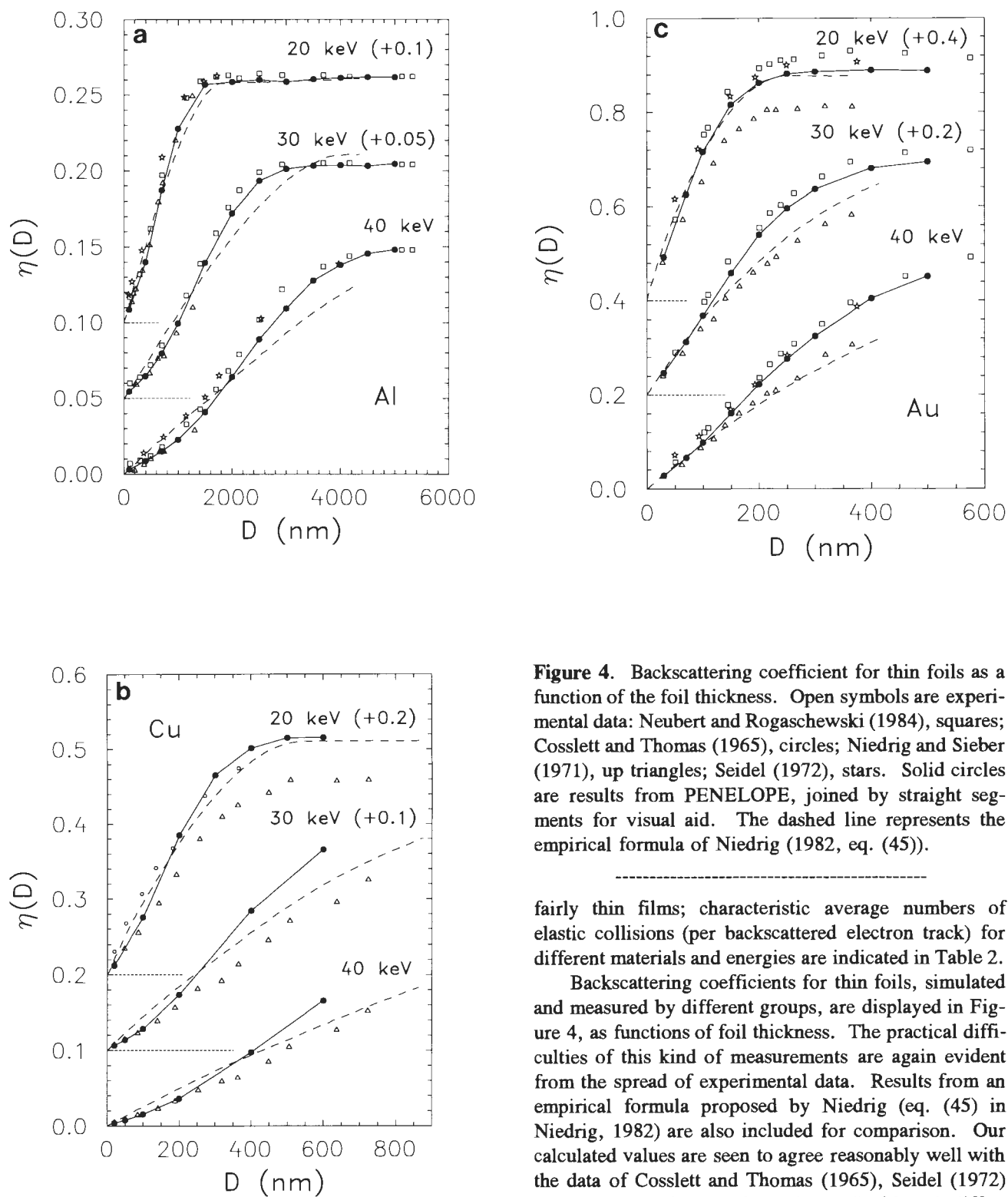
Figure 4. Backscattering coefficient for thin foils as a function of the foil thickness. Open symbols are experimental data: Neubert and Rogaschewski (1984), squares; Cosslett and Thomas (1965), circles; Niedrig and Sieber (1971), up triangles; Seidel (1972), stars. Solid circles are results from PENELOPE, joined by straight segments for visual aid. The dashed line represents the empirical formula of Niedrig (1982, eq. (45)).

----

fairly thin films; characteristic average numbers of elastic collisions (per backscattered electron track) for different materials and energies are indicated in Table 2.

Backscattering coefficients for thin foils, simulated and measured by different groups, are displayed in Figure 4, as functions of foil thickness. The practical difficulties of this kind of measurements are again evident from the spread of experimental data. Results from an empirical formula proposed by Niedrig (eq. (45) in Niedrig, 1982) are also included for comparison. Our calculated values are seen to agree reasonably well with the data of Cosslett and Thomas (1965), Seidel (1972) and Neubert and Rogaschewski (1984) although differences are not always negligible.

Energy distribution of backscattered electrons

The energy distribution of backscattered electrons is of importance in quantitative analysis with EPMA and
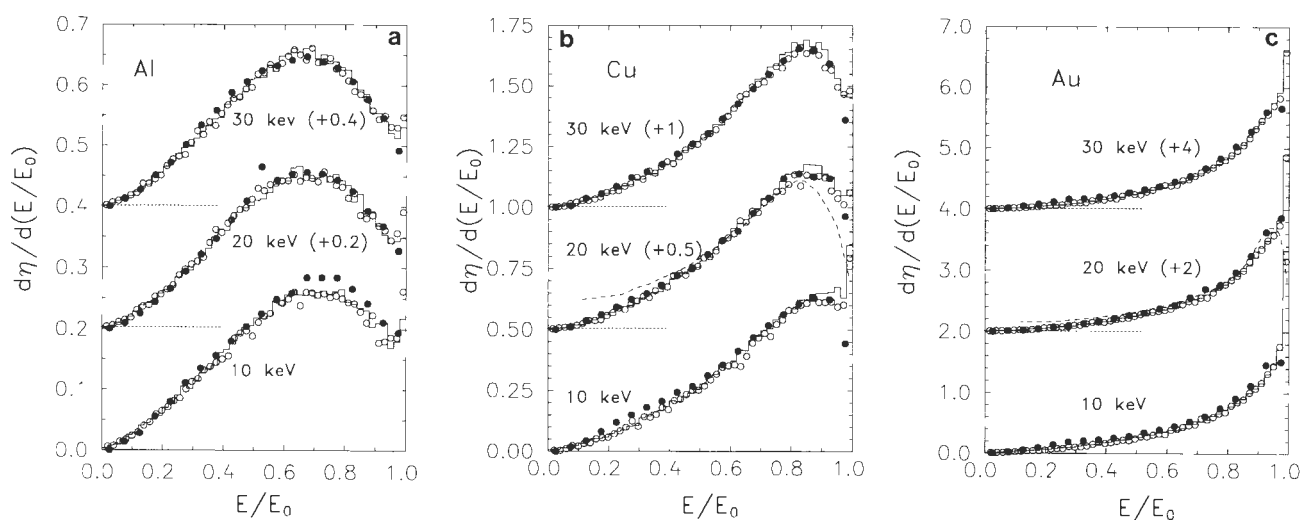
Figure 5. Energy distribution of backscattered electrons as a function of $\epsilon \equiv E/E_0$. Solid circles are experimental data of Darlington (1975) (normalized so as to give the backscattering coefficient obtained by this author). Dashed lines represent measurements by Matsukawa *et al.* (1974). Histograms are results from the detailed simulation code LEEPS of Fernández-Varea *et al.* (1996). Open circles are results generated with PENELOPE.

Table 2. Average number of elastic collisions (N) suffered by the primary electrons backscattered in foils of different thicknesses (D).

E_0(keV)	Al D(mm)	N	Cu D(mm)	N	Ag D(mm)	N	Au D(mm)	N
20	100	24.3	100	63.1	50	34.6	30	24.7
30	400	32.7	50	22.6	50	25.9	30	18.9
40	400	17.9	50	19.3	50	21.5	30	15.6

AES. This distribution enters into empirical calculations of the so-called backscattering correction or *R*-factor. In AES (see, e.g., Merlet *et al.*, 1992), this factor is intended to account for the part of the Auger signal originated by backscattered electrons in their way back to the sample surface. In the case of EPMA (Heinrich and Newbury, 1991), the *R*-factor is defined as the ratio of the number of ionizations actually produced in the specimen to the number that would have been generated if no electrons had been backscattered.

Energy distributions of backscattered electrons for different elemental solids have been measured by Matsukawa *et al.* (1974) and Darlington (1975). Simulation results obtained from PENELOPE are compared with experimental data in Figure 5. The overall agreement is seen to be satisfactory although, owing to the scarcity of measurements, conclusions on the simulation reliability are uncertain from this comparison.

A complementary assessment of the accuracy of PENELOPE regarding energy distributions and other characteristics of backscattering can be inferred from a comparison of the present results with those from a more accurate Monte Carlo code. To this end, simulations have been performed using the recently developed program LEEPS (Fernández-Varea *et al.*, 1996), which performs detailed simulation of electron tracks using accurate DCSs. Elastic scattering is described by means of numerical DCSs calculated by the method of partial waves for a scattering potential that includes exchange and solid-state effects. The DCS for inelastic collisions is obtained from an optical-data model, i.e., from the Born approximation using experimentally determined OOSs, and includes exchange corrections through a modified Ochkur approximation. Fernández-Varea *et al.* (1996) have shown that LEEPS correctly reproduces energy distributions of electrons transmitted through thin

films as measured by electron energy loss spectroscopy (EELS). Typical energy resolutions in EELS experiments are of a few eV and, hence, this kind of experiment provides the most stringent test for the simulation of energy losses. The reliability of the backscattered electron energy distributions generated by LEEPS is evident from Figure 5. It is also clear that PENELOPE yields distributions that are essentially equivalent to those of LEEPS, in spite of the simplifications introduced in the inelastic DCSs.

Conclusions

In conclusion, the scattering model implemented in PENELOPE yields a realistic description of the backscattering of kilovolt electron in solids. We have presented benchmark comparisons with a variety of experimental data, involving materials with different atomic numbers and covering the energy range of interest in surface analytical techniques, from a few keV to 60 keV. Our results agree well with the experiments, in fact as well as those from the much more sophisticated Monte Carlo algorithm LEEPS (Fernández-Varea *et al.*, 1996). Therefore, the use of PENELOPE in practical applications is well justified. Work on quantitative EPMA based on this simulation code is in progress; preliminary results for multilayer specimens have been published elsewhere (Llovet *et al.*, 1996).

Acknowledgements

References

Archard G (1961). Backscattering of electrons. J. Appl. Phys. **32**, 1505-1509.

Baró J, Sempau J, Fernández-Varea JM, Salvat F (1994). Simplified Monte Carlo simulation of elastic electron scattering in limited media. Nucl. Instrum. Meth. B **84**, 465-483.

Baró J, Sempau J, Fernández-Varea JM, Salvat F (1995). Penelope: An algorithm for Monte Carlo simulation of the penetration and energy loss of electrons and positrons in matter. Nucl. Instrum. Meth. B **100**, 31-46.

Berger MJ (1963). Monte Carlo calculation of the penetration and diffusion of fast charged particles. In: Methods in Computational Physics, vol. 1. Alder B, Fernbach S, Rotenberg M (eds.). Academic Press, New York. pp. 135-215.

Berger MJ, Seltzer SM (1982). Stopping Powers and Ranges of Electrons and Positrons. NBSIR 82-2550-A. National Bureau of Standards, Gaithersburg, MD. Also available as ICRU report 37 (1984), International Commission on Radiation Units and Measurements, Bethesda, MD.

Berger MJ, Seltzer SM (1988). The ETRAN system. In: Monte Carlo Transport of Electrons and Photons. Jenkins TM, Nelson WR, Rindi A (eds.). Plenum Press, New York. Chapters 7-9, pp. 153-246.

Bielajew AF, Rogers D (1987). PRESTA: The parameter reduced electron-step transport algorithm for electron Monte Carlo transport. Nucl. Instrum. Meth. B **18**, 165-181.

Bielajew AF, Rogers D (1988). Variance-reduction techniques. In: Monte Carlo of Electrons and Photons. Jenkins TM, Nelson WR, Rindi A (eds.). Plenum Press, New York. Chapter 18, pp. 407-419.

Cosslett V, Thomas R (1965). Multiple scattering of 5-30 keV electrons in evaporated metal films III: Backscattering and absorption. Br. J. Appl. Phys. **16**, 779-795.

Darlington E (1975). Backscattering of 10-100 keV electrons from thick targets. J. Phys. D: Appl. Phys. **8**, 85-93.

Drescher H, Reimer L, Seidel H (1970). Backscattering and secondary electron emission of 10 to 100 keV electrons and correlations to scanning electron microscopy. Z. Angew. Phys. **29**, 331-336.

Everhart T (1960). Simple theory concerning the reflection of electrons from solids. J. Appl. Phys. **31**, 1483-1490.

Fathers D, Rez P (1979). A transport equation theory of electron backscattering. Scanning Electron Microsc. **1979**; I, 55-66.

Fernández-Varea JM, Martínez JD, Salvat F (1991). A simplified method for the detailed Monte Carlo simulation of electron transport. J. Phys. D: Appl. Phys. **24**, 814-826.

Fernández-Varea JM, Mayol R, Baró J, Salvat F (1993). On the theory and simulation of multiple elastic scattering of electrons. Nucl. Instrum. Meth. B **73**, 447-473.

Fernández-Varea JM, Liljequist D, Csillag S, Räty R, Salvat F (1996). Monte Carlo simulation of 0.1-100 keV electron and positron transport in solids using optical data and partial wave methods. Nucl. Instrum. Meth. B **108**, 35-50.

Heinrich KFJ, Newbury DE (eds.) (1991). Electron Probe Quantitation. Plenum Press, New York. pp. 177-

190.

Hunger H, Küchler L (1979). Measurements of the electron backscattering coefficient for quantitative electron probe microanalysis in the energy range of 4 to 40 keV. Phys. Stat. Sol. (a) **56**, K45-K48.

Inokuti M (1971). Inelastic collisions of fast charged particles with atoms and molecules-the Bethe theory revisited. Rev. Mod. Phys. **43**, 297-347.

Jenkins TM, Nelson WR, Rindi A (eds.) (1988). Monte Carlo Transport of Electrons and Photons. Plenum Press, New York. Chapters 7-14.

Kalos MH, Whitlock PA (1986). Monte Carlo Methods, vol. 1. Wiley, New York. Chapter 6.

Kanter H (1957). On the backscattering of electrons in the energy range from 10 to 100 keV. Ann. Phys. **20**, 144-166.

Lederer CM, Shirley VS (eds.) (1978). Tables of Isotopes, 7th edition. Wiley, New York. Appendix III.

Liljequist D (1983a). A discussion of the parameters of primary importance in plural and multiple electron scattering and energy loss. Scanning Electron Microsc. **1983**; III, 1019-1033.

Liljequist D (1983b). A simple calculation of inelastic mean free path and stopping power for 50 eV-50 keV electrons in solids. J. Phys. D: Appl. Phys. **16**, 1567-1582.

Llovet X, Riveros JA, Salvat F (1996). Application of a new Monte Carlo simulation algorithm to electron probe microanalysis. Mikrochim. Acta (in press).

Martínez JD, Mayol R, Salvat F (1990). Monte Carlo simulation of kilovolt electron transport in solids. J. Appl. Phys. **67**, 2955-2964.

Massoumi G, Hozhabri N, Lennard W, Schultz P (1991). Doubly differential positron backscattering yields. Phys. Rev. B **44**, 3486-3489.

Matsukawa T, Shimizu R, Hashimoto H (1974). Measurements of the energy distribution of backscattered kilovolt electrons with a spherical retarding-field energy analyser. J. Phys. D: Appl. Phys. **7**, 695-702.

Merlet C, Jbara O, Rondot S, Cazaux J (1992). Auger backscattering factor at primary beam energies above 10 keV. Surf. Interf. Anal. **19**, 192-196.

Nakhodin N, Ostroukhov A, Romanovskii V (1962). Electron inelastic scattering in thin films. Soviet Physics-Solid State **4**, 1112-1119.

Nelson WR, Hirayama H, Rogers DWO (1985). The EGS4 Code System. Stanford Linear Accelerator Center Report No. SLAC-265. Stanford, California.

Neubert G, Rogaschewski S (1980). Backscattering coefficient measurements of 15-60 keV electrons in solids at various angles of incidence. Phys. Stat. Sol. (a) **59**, 35-41.

Neubert G, Rogaschewski S (1984). Measurements of the back-scattering and absorption of 15-60 keV electrons for transparent solid films at various angles of incidence. J. Phys. D: Appl. Phys. **17**, 2439-2454.

Niedrig H (1981). Simple theoretical models for electron backscattering from solid films. Scanning Electron Microsc. **1981**; I, 29-45.

Niedrig H (1982). Electron backscattering from thin films. J. Appl. Phys. **53**, R15-R49.

Niedrig H, Sieber P (1971). Backscattering of fast electrons by thin foils. Z. Angew. Phys. **31**, 27-37.

Reimer L, Krefting E (1976). The effect of scattering models on the results of Monte Carlo calculations. In: Proceedings of the Workshop on Use of Monte Carlo Calculations in Electron Probe Microanalysis and Scanning Electron Microscopy, Gaithersburg. NBS Special Publ. 460. US Gov. Printing Office, Washington DC [now available from National Technical Information Service (NTIS), Alexandria, VA]. pp. 45-60.

Salvat F, Fernández-Varea JM (1992). Semiempirical cross sections for the simulation of the energy loss of electrons and positrons in matter. Nucl. Instrum. Meth. B **63**, 255-269.

Salvat F, Mayol R (1993). Elastic scattering of electrons and positrons by atoms. Schrödinger and Dirac partial wave analysis. Comput. Phys. Commun. **74**, 358-374.

Salvat F, Martinez JD, Mayol R, Parellada J (1987). Analytical Dirac-Hartree-Fock-Slater screening functions for atoms (Z = 1-92). Phys. Rev. A **36**, 467-474.

Seidel H (1972). Measurements of backscattering and transmission coefficients of poly-crystalline materials and on the orientation dependence of the backscattering coefficient and of the secondary electron yield for 9 to 100 keV electrons. Doctoral Thesis, University of Münster. Germany.

Shimizu R, Murata K (1971). Monte Carlo calculations of the electron-sample interactions in the scanning electron microscope. J. Appl. Phys. **42**, 387-394.

Sternheimer RM (1952). The density effect for the ionization loss in various materials. Phys. Rev. **88**, 851-859.

Sternheimer RM, Berger MJ, Seltzer SM (1984). Density effect for the ionization loss of charged particles in various substances. Atom. Data Nucl. Data Tables **30**, 261-271.

Thümmel H (1974). Passage of Electrons and Beta Rays Through Films of Matter. Akademie-Verlag, Berlin, German Democratic Rep. Chapters 9-11.

Discussion with Reviewers

M. Dapor: Vicanek and Urbassek (1991) have recently suggested that the backscattering coefficient of light ions is a simple function of the ratio between the range and

the transport mean free path. According to their theory, in other words, the backscattering coefficient essentially depends on the mean number of large-angle collisions suffered by the particles before slowing down to rest. Can you give a comment regarding the importance of the transport cross section in backscattering yield determination?

Authors: As for elastic scattering, the backscattering yield results from a delicate balance between single large-angle collisions and multiple small-angle scattering. The global effect is primarily governed by the transport cross section or, more precisely, by the mentioned ratio if energy loss is considered (see, e.g., Liljequist, 1983a). Indeed, in order to have the correct angular deflection per unit path length, the W2D DCS implemented in PENELOPE uses transport mean free path values obtained from accurate partial-wave calculations.

K. Murata: Have you checked whether your model predicts appropriate results for the angular distribution of backscattered electrons?

Authors: For thick samples, the angular distribution of backscattered electrons is smooth and rather structureless, and is nearly reproduced by any sound scattering model. A more stringent test of the elastic scattering model is provided by the angular distribution of electrons ejected from the sample after one (or a few) elastic collisions with small energy loss or by the angular distributions of electrons transmitted through thin foils. However, as PENELOPE yields reliable results only under multiple scattering conditions, discrepancies between experiment and simulation results are to be expected for these extreme cases.

K. Murata: We can see a very high peak in the energy distribution of backscattered electrons near the incident energy, especially for high atomic number materials and low energies, which is not seen in the experimental results. Could you comment on how the peak is yielded and the validity of your simulation?

Authors: This peak is due to electrons that are backscattered after a single large-angle elastic collision (possibly combined with plural small-angle interactions) with small energy loss. This quasi-elastic peak is also obtained with the much more sophisticated code LEEPS and in experiments (see, e.g., Jablonski *et al.*, 1989). The absence of such a quasi-elastic peak in the experimental results of Darlington (1975) is likely due to poor energy resolution. The agreement between energy distributions generated by LEEPS and PENELOPE provides a clear indication of the validity of the latter code.

D.E. Newbury: Consider a simple vertical planar boundary between two materials of different composi-

tion. How will your simulation handle the problem of boundary crossing?

Authors: As mentioned in the text, PENELOPE has been devised to work for complex geometries. Interface crossings are handled as in purely detailed simulations, i.e., when the particle arrives at a surface separating two media with different composition, it is stopped just after the interface, and simulation is continued using the scattering data of the new medium. For purely detailed simulation, this procedure is justified by the Markovian character of the interaction process. In the case of mixed simulation, the algorithm implemented in PENELOPE properly accounts for the average effect of soft (elastic and inelastic) interactions along the step that ends at the boundary (see Baró *et al.*, 1995).

D.E. Newbury: The description of the PENELOPE model seems to consider only pure element targets. Please describe explicitly how you incorporate multiple elements into your Monte Carlo calculation, for example, if a compound such as GaP or GaAs is to be simulated.

Authors: Regarding elastic scattering, the simulation of compounds is performed by using a molecular DCS equal to the sum of the atomic DCS of all atoms in a molecule (additivity approximation). In other words, the integrated cross sections (9)-(11) per molecule are obtained by adding the corresponding values of the atoms present. The inelastic DCS is formally the same as for single elements, i.e., the GOS is given by eq. (3), but now the summation runs over the bound shells of the different atoms and the mean excitation energy I adequate to the compound must be used. Thus, the simulation of compounds proceeds along the same lines as for pure elements.

P. Rez: One can produce a curve like Figure 2 (backscattering as function of kV) using a number of different (and contradictory) theoretical models. The key parameter appears to be the ratio of elastic to inelastic scattering. Would the authors like to comment on how significant this ratio is for all backscattering measurements?

Authors: Yes. It seems that the ratio $r(E_0)$ of the transport mean free path to the continuous slowing down approximation range, evaluated for the initial electron energy E_0, practically determines the backscattering coefficient (see the discussion in Liljequist, 1983a). If this ratio remains constant for decreasing energies, simulated electron trajectories obey a simple linear scaling law, which implies that the backscattering coefficient is independent of E_0. However, such an idealized "linear" process has only a limited validity since it is incompatible with the observed energy dependence of the back-

scattering coefficient. Possibly, a detailed analysis of the energy dependence of the ratio $r(E)$ would permit a qualitative understanding of this experimental fact. On the other hand, when η is nearly energy independent (as it seems to happen for more or less wide energy intervals depending on the atomic number), the aforementioned scaling property of electron tracks implies that angular and energy distributions (the latter as a function of E/E_0) of backscattered electrons are also approximately independent of E_0.

P. Rez: In a more sophisticated view of inelastic scattering, the cross sections would be derived from measured optical oscillator strengths. Do the authors think that this would be necessary for low voltage electrons? Are they worried about the neglect of exchange (in both elastic and inelastic scattering) at low energies?

Authors: Certainly, the use of more accurate inelastic DCSs for low energies would be required to obtain energy distributions with high resolutions, of the order of 100 eV or less, not only for low-voltage electrons. The discrete nature of the OOS used in PENELOPE will show up when the number of inelastic collisions is small (thin samples), but it is smeared out after multiple inelastic scattering. We would like to stress the fact that the whole simulation algorithm has been tailored to be as simple as possible and still yield accurate results *under multiple scattering conditions.* When these are not satisfied, one should use more realistic inelastic scattering models, based on measured optical oscillator strengths, such as those implemented in LEEPS. Exchange effects have been approximately accounted for by means of simple approximations. The integrated elastic cross sections, eqs. (9)-(11) were obtained from partial wave calculations for the electrostatic field of the target atom plus the local exchange field proposed by Furness and McCarty (1973), exchange corrections are negligible for $E > 5$ keV. In the case of inelastic scattering, exchange effects are introduced only for close collisions (i.e., those on the Bethe ridge). These are described by using the (relativistic) Moller DCS instead of the Rutherford DCS. This correction is essential to obtain the correct energy-dependence of the stopping power at high energies.

R. Gauvin: Explain how your elastic cross sections are different to those computed by Czyzewski *et al.* (1990) since those cross sections are readily available to the authors under request.

Authors: The atomic potentials underlying our elastic cross section calculations and those used by Czyzewski *et al.* (1990) are similar (self-consistent free-atom fields of comparable accuracy). However, we disregard solid-state effects, which are accounted for within the muf-

fin-tin approximation by Czyzewski *et al.* (1990), and include electron-exchange effects by means of a local approximate potential (see Salvat and Mayol, 1993). The PWADIR code (which is obtainable from the CPC program Library, Queen's University of Belfast, N. Ireland) permits the calculation of accurate elastic cross sections for energies up to about 1 MeV, whereas the tabulation of Czyzewski *et al.* (1990) is limited to the energy range 20 eV to 20 keV.

R. Gauvin: From the compilation of David C. Joy about experimental measurements of electron backscattering coefficient, more data are available for Au and C than those presented in Figure 1. Since variations of 50% are common for measurements below 3 keV, it seems very difficult to validate any Monte Carlo code since experimental measurements are generally inaccurate owing to beam current fluctuations, surface roughness and contamination which are more important at low energy. Also, the more we find experimental data, the more we observe scatter. So, since your simulations agree well with few experimental points, can we expect more disagreement when more experimental points will become available?

Authors: We certainly agree in that benchmark comparisons with measured backscattering coefficients do not provide the ultimate test of the validity of a Monte Carlo code. However, assuming that experimental uncertainties are of a random nature, it seems sensible to conclude that a code which provides an *average* description of the data should be trustworthy. It would be desirable to have many data, from different laboratories, for the same materials and energies, since then a statistical analysis of these would yield an estimate that is more reliable than the separate data.

R. Gauvin: You claim that analytical equations are faster to compute cross sections than interpolation in a data base. This depends on the way the table and the interpolation scheme are programmed. We have found that interpolation is faster than simple analytical equations (Browning *et al.*, 1995) when clever techniques of programation are used.

Authors: We agree that total elastic cross section can be computed faster by interpolation than from analytical formulae. Indeed, in PENELOPE σ_{el} (as well as other energy-dependent quantities) is obtained by interpolation. Our claim, however, refers to the sampling of the scattering angle from the differential cross section. In LEEPS we use a purely numerical, accurate and efficient sampling algorithm from Mott's differential cross section; the one implemented in PENELOPE is faster and yields essentially the same angular distributions (provided the number of scattering events is statistically

sufficient).

P. Hovington: What is the cutoff energy values you are using to transfer to and from detailed simulations? Is it a function of E and Z?

Authors: The cutoff energies are selected by the user in such a way that multiple scattering conditions are satisfied, i.e., at least about 15 inelastic interactions must occur on average along an electron trajectory (in thin layers this minimum number may not be reached). In the present simulations, a value of 100 eV was adopted to separate "hard" from "soft" inelastic collisions. Notice that this value is also smaller than the width of the bins used to tally energy distributions of backscattered electrons.

D. Liljequist: The values of the coefficients $a_1(Z)$ and $a_2(Z)$, eq. (13), seem to be regularly varying with atomic number Z. Is it possible to make a fit also to the variation of these coefficients with Z - at least to some specified accuracy? This would give a good practical formula in E and Z. As a difficulty in this respect, the authors point to fluctuations in the dependence on Z, but these fluctuations do seem rather small to me (Fig. 2); should they not be next to negligible in the first approximation, bearing in mind the spread of the experimental data?

Authors: Actually, the original idea concerning this issue was to obtain an analytical expression for η as a function of E_0 and Z. After fitting the coefficients in eq. (13) as functions of Z, we observed that the dependence was not smooth and severe discontinuities appeared. As a result of this feature, the values of the backscattering coefficient could not be reproduced. In fact, different functional dependencies were essayed for $\eta(E_0,Z)$, and the same problem arose for them all.

D. Liljequist: The simulations are claimed to predict a partial but not negligible fluctuating (non-smooth) dependence of the bulk backscattering on Z at a given incident energy. This observation is interesting, but is there any significant experimental evidence to support it? Again, the fluctuations in Figure 2 seem very small to me.

Authors: The fluctuations in the Z dependence of η given by simulated data are indeed small at $E_0 = 30$ keV, but they are larger than the statistical uncertainties of simulated values. It should also be noted that larger fluctuations are expected for lower energies. As the spread of experimental data in Figure 2 is greater than these fluctuations, no experimental evidence can be provided unless a more accurate experimental database is available.

D. Liljequist: A very good point is made by the authors when they argue that the spread of experimental data indicates the presence of "instrumental uncertainties" (including sample preparation, etc.) and that, therefore, a comparison with measurements from a single laboratory may not be conclusive. Not only can one suspect some experimental results to be in "error", but quite fortuitous agreement may also occur. The reliability of a code is thus, as regards benchmark comparisons, limited by the spread among the (unfortunately rather few) available experimental data. If theoretically believed to be accurate, the code may be regarded as a prediction, awaiting future tests. If, finally, accuracy is regarded as desirable for a particular application, should not this application be possible to use as a more stringent test? Do the authors have some further comment on this, with regard to the expected accuracy of their code?

Authors: As already mentioned, PENELOPE is a general-purpose code which can be applied from about 1 keV to several hundred MeV, provided multiple scattering conditions are fulfilled. Applications to electron probe microanalysis, detector response characterization, and medical electron-beam dosimetry are currently in progress. These applications cover different energy ranges and, in general, we find very good agreement with experiments. It is on the basis of this agreement that we are confident about the global accuracy of the code.

Additional References

Browning R, Li TZ, Chui B, Jun Ye, Pease RFW, Czyzewski Z, Joy DC (1995). Low-energy electron/atom elastic scattering cross sections from 0.1-30 keV. Scanning **17**, 250-253.

Czyzewski Z, O'Neill MacCallum D, Romig A, Joy D (1990). Calculations of Mott scattering cross section. J. Appl. Phys. **68**, 3066-3072.

Furness JB, McCarty IE (1973). Semiphenomenological optical model for electron scattering on atoms. J. Phys. B **6**, 2280-2291.

Jablonski A, Gryko J, Kraar J, Tougaard S (1989). Elastic electron backscattering from surfaces. Phys. Rev. B **39**, 61-71.

Vicanek M, Urbassek H (1991). Reflection coefficient of low-energy light ions. Phys Rev B **44**, 7234-7242.